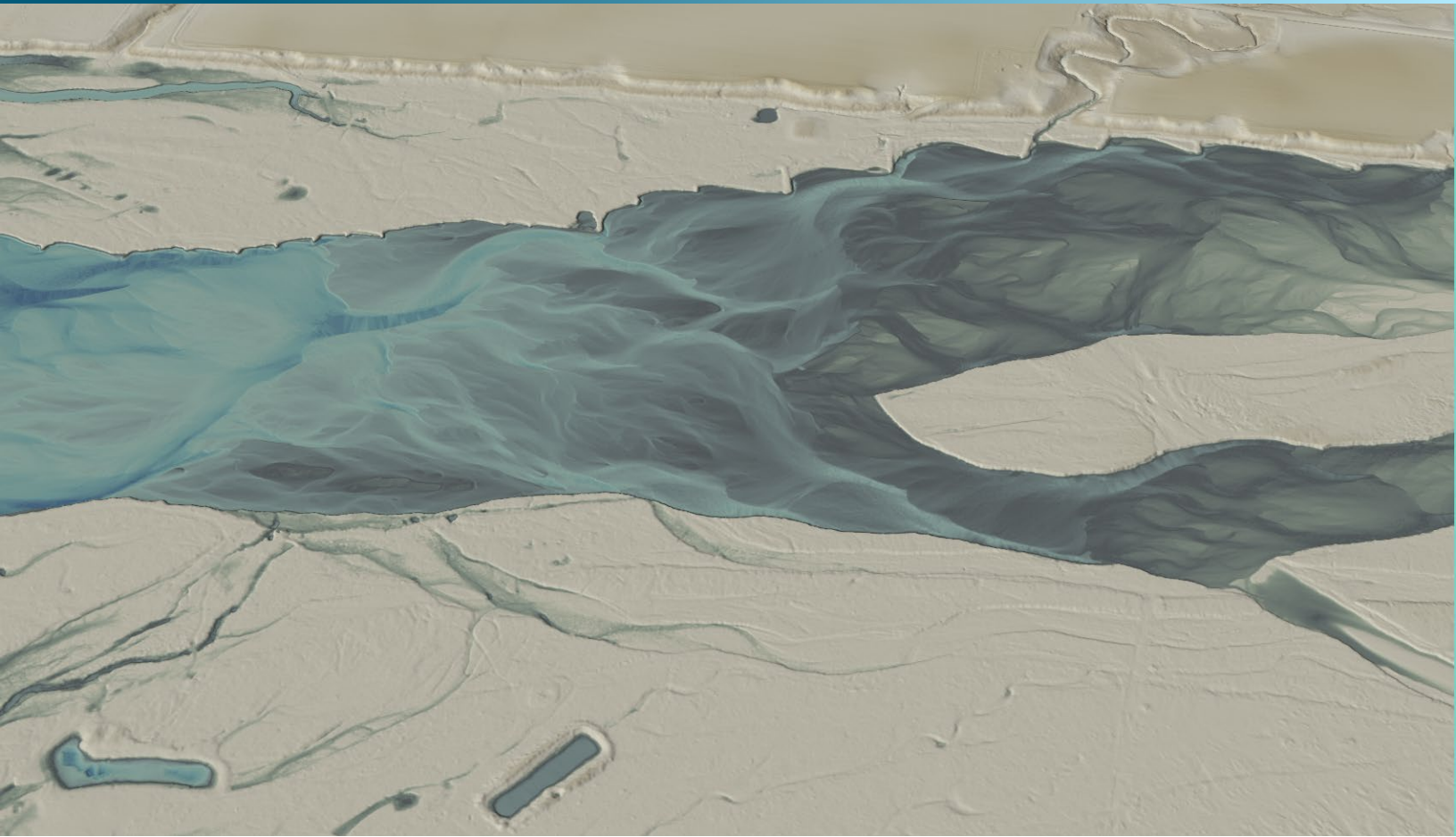


March 06, 2023



Lower Platte River, Nebraska

2022 Topobathymetric Lidar Technical Data Report

Prepared For:



Headwaters Corporation

Platte River Recovery Implementation Program
Jason Farnsworth, Executive Director
4111 4th Avenue, Suite 6
Kearney, Nebraska 68845
PH: 308-237-5728

Prepared By:



NV5 Geospatial Corvallis

1100 NE Circle Blvd, Ste. 126
Corvallis, OR 97330
PH: 541-752-1204

TABLE OF CONTENTS

INTRODUCTION	1
Deliverable Products	2
ACQUISITION	4
Planning	4
Turbidity Measurements and Secchi Depth Readings	4
Airborne Lidar Survey	8
Ground Survey	11
Base Stations	11
Ground Survey Points (GSPs)	11
PROCESSING	14
Topobathymetric Lidar Data	14
Bathymetric Refraction	17
Lidar Derived Products	17
Topobathymetric DEMs	17
Intensity Images	18
Feature Extraction	19
Hydroflattening and Water's edge breaklines	19
RESULTS & DISCUSSION	20
Bathymetric Lidar	20
Mapped Bathymetry and Depth Penetration	20
Lidar Point Density	22
First Return Point Density	22
Bathymetric and Ground Classified Point Densities	22
Lidar Accuracy Assessments	25
Lidar Non-Vegetated Vertical Accuracy	25
Lidar Bathymetric Vertical Accuracies	27
Lidar Relative Vertical Accuracy	29
Lidar Horizontal Accuracy	30
CERTIFICATIONS	31
SELECTED IMAGES	32
GLOSSARY	33
APPENDIX A - ACCURACY CONTROLS	34

Cover Photo: A view looking south at the Lower Platte River. The image was created from the lidar bare earth model colored by elevation.

LIST OF FIGURES

Figure 1: Location map of the Lower Platte River site in Nebraska	3
Figure 2: USGS Station 06796000 gage height along the Platte River at the time of lidar acquisition.	6
Figure 3: USGS Station 06796000 gage height along the Platte River at the time of lidar acquisition.	6
Figure 4: These photos, taken by NV5 acquisition staff, display water clarity conditions within the Lower Platte River site.	7
Figure 5: Flightlines map.....	10
Figure 6: Ground survey location map	13
Figure 7: A comparison of Intensity Images from Green and NIR first returns in the Lower Platte River area.....	18
Figure 8: Example of hydroflattening in the Lower Platte River dataset	19
Figure 9: Depth model of the Skagit River.....	21
Figure 11: Frequency distribution of first return densities per 100 x 100 m cell.....	23
Figure 12: Frequency distribution of ground and bathymetric bottom classified return densities per 100 x 100 m cell.....	23
Figure 17: First return and ground and bathymetric bottom density map for the Lower Platte River site (100 m x 100 m cells).....	24
Figure 14: Frequency histogram for classified LAS deviation from ground check point values	26
Figure 15: Frequency histogram for lidar bare earth DEM deviation from ground check point values.....	26
Figure 16: Frequency histogram for lidar surface deviation ground control point values	27
Figure 17: Frequency histogram for lidar surface deviation from submerged check point values	28
Figure 18: Frequency histogram for lidar surface deviation from wetted edge check point values	28
Figure 19: Frequency plot for relative vertical accuracy between flight lines.....	29
Figure 20: View looking east over Lower Platte River. The image was created from the lidar bare earth model overlaid with the above-ground point cloud.	32

LIST OF TABLES

Table 1: Acquisition dates, acreage, and data types collected on the Lower Platte River site.....	2
Table 2: Deliverable product coordinate reference system information	2
Table 3: Lidar and imagery products delivered for the Lower Platte River site.....	2
Table 4: 2022 Water Clarity Observations for Lidar flights.....	5
Table 5: Lidar specifications and survey settings	8
Table 6: Base station positions for the Lower Platte River acquisition. Coordinates are on the NAD83 (2011) datum, epoch 2010.00.....	11
Table 7: NV5 Geospatial ground survey equipment identification	12
Table 8: ASPRS LAS classification standards applied to the Lower Platte River dataset	15
Table 9: Lidar processing workflow	16
Table 10: Average Lidar point densities.....	22
Table 11: Absolute accuracy results	25
Table 12: Bathymetric Vertical Accuracy for the Lower Platte River Project	27
Table 13: Relative accuracy results	29
Table 14: Horizontal Accuracy.....	30

INTRODUCTION

This photo, taken by NV5 acquisition staff, shows a view of the Lower Platte River site in Nebraska.



In June 2020, NV5 Geospatial (NV5) was contracted by Headwaters Corporation to collect topobathymetric Light Detection and Ranging (lidar) data in the summer of 2022 during leaf-on conditions for the Lower Platte River site in eastern Nebraska. Traditional near-infrared (NIR) lidar was fully integrated with green wavelength (bathymetric) lidar in order to provide a seamless topobathymetric lidar dataset for analysis. This type of lidar data is well-suited for use in riverine locations, and is useful for assessing channel morphology and accurately modeling the topobathymetric surface inside of the study area.

This report pertains to an area of the Platte River that extends from the confluence with the Missouri River, upriver to just west of its fork with the Loup River. This area was planned as a one-time acquisition. It is located east of the standard area for Platte River that has been annually surveyed by NV5 Geospatial for the Headwaters Corporation as part of the Platte River Recovery Implementation Program. The area encompassing this Lower Platte River dataset had generally higher turbidity and more islands when compared to previous Platte River datasets collected for Headwaters. This data collection is a part of NV5 Geospatial's partnership with Headwaters Corporation to provide data aiding in the Platte River Recovery Implementation Program. The Program is aimed at enhancing, restoring, and protecting the habitat for endangered species associated with the river system, specifically targeting the whooping crane, least tern, piping plover, and pallid sturgeon species.

This report accompanies the delivered topobathymetric lidar data and documents contract specifications, data acquisition procedures, processing methods, and analysis of the final dataset including lidar accuracy, depth penetration, and density. Acquisition dates and acreage are shown in, a complete list of contracted deliverables provided to Headwaters Corporation is shown in Table 3 with the coordinate reference system information for these deliverables shown in Table 2, and the project extent is shown in Figure 1.

Table 1: Acquisition dates, acreage, and data types collected on the Lower Platte River site

Project Site	Contracted Acres	Buffered Acres	Acquisition Dates	Data Type
Lower Platte River, Nebraska	74,826	83,670	08/17/2022 - 8/23/2022	Topobathymetric - Lidar

Deliverable Products

Table 2: Deliverable product coordinate reference system information

Projection	Horizontal Datum	Vertical Datum	Units
Nebraska State Plane	NAD83(2011)	NAVD88(GEOID03)	US Survey Feet

Table 3: Lidar and imagery products delivered for the Lower Platte River site

Product Type	File Type	Product Details
Points	LAS v.1.4 (*.las)	<ul style="list-style-type: none"> All Classified Returns
Rasters	3.0 Foot ERDAS Imagine Files (*.img)	<ul style="list-style-type: none"> Tiled: <ul style="list-style-type: none"> Void-Interpolated Topobathymetric Bare Earth Digital Elevation Model (DEM) Void-Clipped Topobathymetric Bare Earth Digital Elevation Model (DEM) Mosaic: <ul style="list-style-type: none"> Void-Interpolated Topobathymetric Bare Earth Digital Elevation Model (DEM) Void-Clipped Topobathymetric Bare Earth Digital Elevation Model (DEM) Hydro-flattened Bare Earth Digital Elevation Model (DEM) Highest Hit Digital Surface Model (DSM)
Rasters	1.5 foot GeoTIFFs (*.tif)	<ul style="list-style-type: none"> Green Sensor Intensity Images NIR Sensor Intensity Images
Vectors	Shapefiles (*.shp)	<ul style="list-style-type: none"> Area of Interest Tile Index Flightlines Ground Survey Points Water's Edge Breaklines Submerged Topography Density

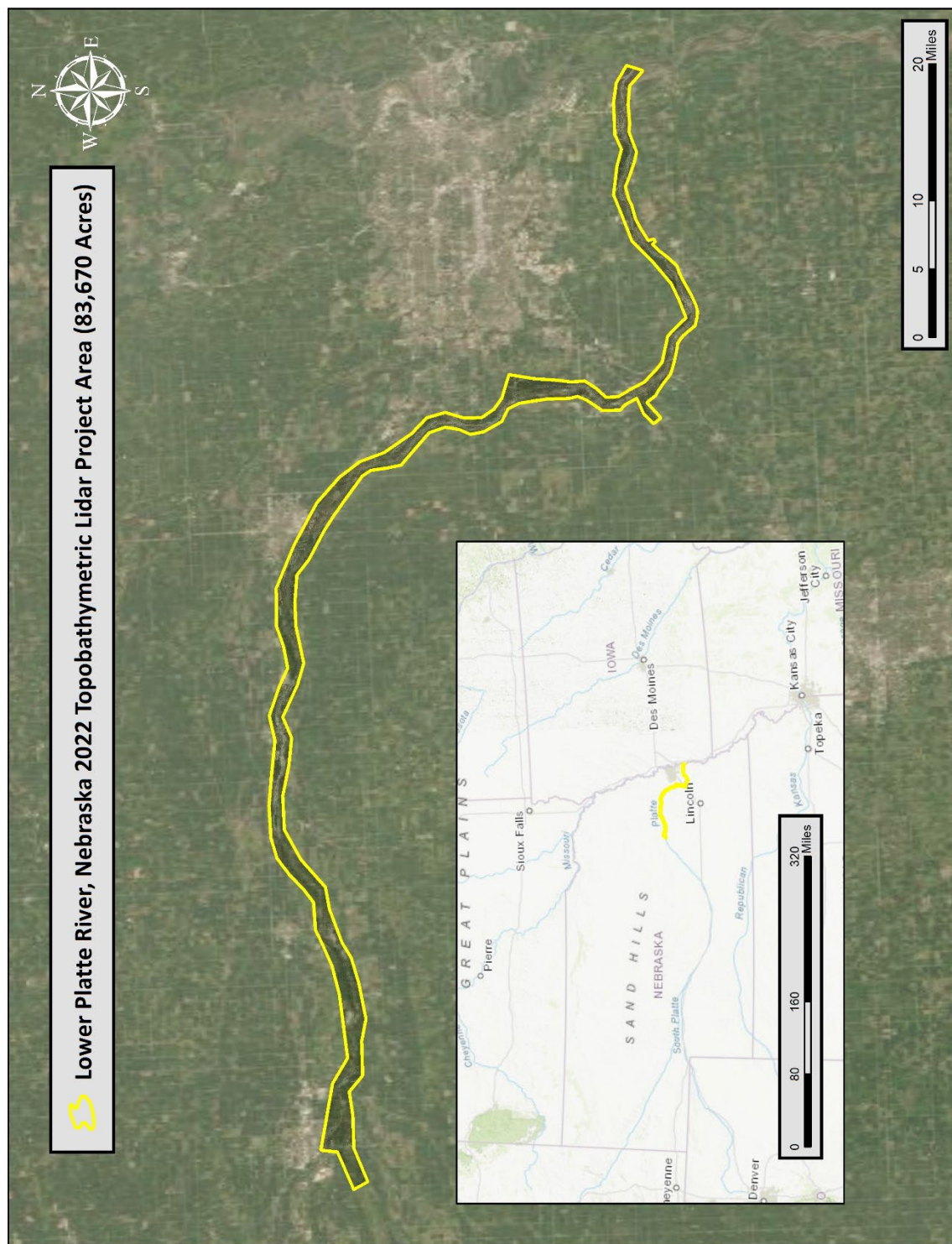


Figure 1: Location map of the Lower Platte River site in Nebraska

ACQUISITION

NV5's ground acquisition equipment set up in the Lower Platte River Lidar study area.



Planning

In preparation for data collection, NV5 reviewed the project area and developed a specialized flight plan to ensure complete coverage of the Lower Platte River Lidar study area at the target combined point density of ≥ 6 points/m². Acquisition parameters including orientation relative to terrain, flight altitude, pulse rate, scan angle, and ground speed were adapted to optimize flight paths and flight times while meeting all contract specifications. Figure 5 shows these optimized flight paths and dates.

Factors such as satellite constellation availability and weather windows must be considered during the planning stage. Any weather hazards or conditions affecting the flight were continuously monitored due to their potential impact on the daily success of airborne and ground operations. In this particular area, acquisition and processing were planned around a control dam that causes the water to fill up during the night and drop during the day to ensure that the water levels weren't drastically different. In addition, logistical considerations including private property access, potential air space restrictions, channel flow rates (Figure 2 and Figure 3) and water clarity were reviewed.

Turbidity Measurements and Secchi Depth Readings

In order to assess water clarity conditions prior to and during lidar and digital imagery collection, NV5 collected turbidity measurements, secchi depth readings, and wind speed and direction measurements. Readings were collected at twelve locations throughout the project site between August 18th to 23rd, 2022. Turbidity and wind observations were recorded twice to confirm measurements. Table 4 below provides turbidity and secchi depth results per site on each day of data collection. A true Secchi depth reading is where the Secchi depth reaches extinction. However, because of safety concerns and accessibility, all secchi depth readings were noted to have reached the bottom surface of the riverbed.

Table 4: 2022 Water Clarity Observations for Lidar flights

Date	Time (UTC -7h)	Location	Turbidity Read 1 (NTU)	Turbidity Read 2 (NTU)	Turbidity Read 3 (NTU)	*Secchi Depth (m)	Wind Speed/direction (knots)
8/18	17:20	downstream of the Platte and Loup River confluence, and Southeast of Columbus, NE	30.73	29.04	30.20	*0.50	4.9 E
8/19	10:52	immediately East of Highway 15, and South of Schuyler, NE	16.93	15.11	16.65	0.50	1.9 E
8/19	12:40	South-West of North Bend, NE	29.24	31.55	31.64	0.30	5.8 with 6.2 E gusts
8/20	10:32	one mile South of Highway 30, and 3 miles Southeast of North Bend, NE	22.58	20.72	21.40	*0.50	6.7 with 10.2 N gusts
8/20	12:55	1.5 miles South of Highway 30, 7 miles Southeast of North Bend, NE and 8 miles west of Fremont, NE	16.30	15.22	15.69	*0.26	1.2 with 2.3 N gusts
8/20	14:59	0.75miles South of Highway 30, and 4 miles west of Fremont, NE	13.33	9.81	11.53	*0.40	3.8 with 5.2 N gusts
8/21	10:40	two miles South of Old US Highway 275 and Fremont, NE	30.97	26.99	26.13	*0.24	1.2 with 1.7 NE gusts
8/21	13:41	immediately north of Ida Street (State Highway 64) and west of Platte River State Access	34.13	36.53	37.99	0.35	6.9 with 8.6 NE gusts
8/21	15:40	0.5 miles north of State Highway 92	43.24	42.79	43.82	*0.15	3.6 with 6.8 N gusts
8/22	11:23	directly West of Biel Dike Road and East of County Road E. 5 miles South-West of Gretna, NE	19.82	17.49	19.03	*0.33	0.4 with 0.8 SE gusts
8/22	14:00	directly West of Interstate 80 and North of Plattevale Drive. 4 miles Southeast of Ashland, NE	38.10	37.83	35.02	0.30	1.2 with 1.9 N
8/23	10:00	directly East of State Highway 50 and South of State Highway 31. One mile North of Louisville, NE	38.65	42.15	37.90	0.30	0 with 1.9 W

* Measurement is depth to the bottom surface due to observational depth limitations

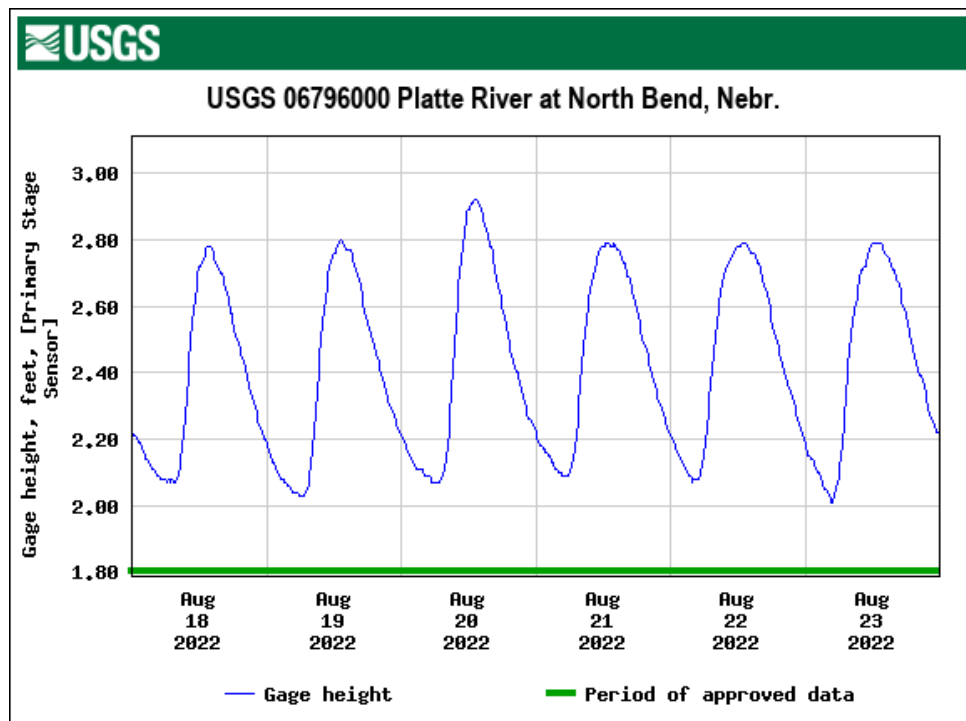


Figure 2: USGS Station 06796000 gage height along the Platte River at the time of lidar acquisition.

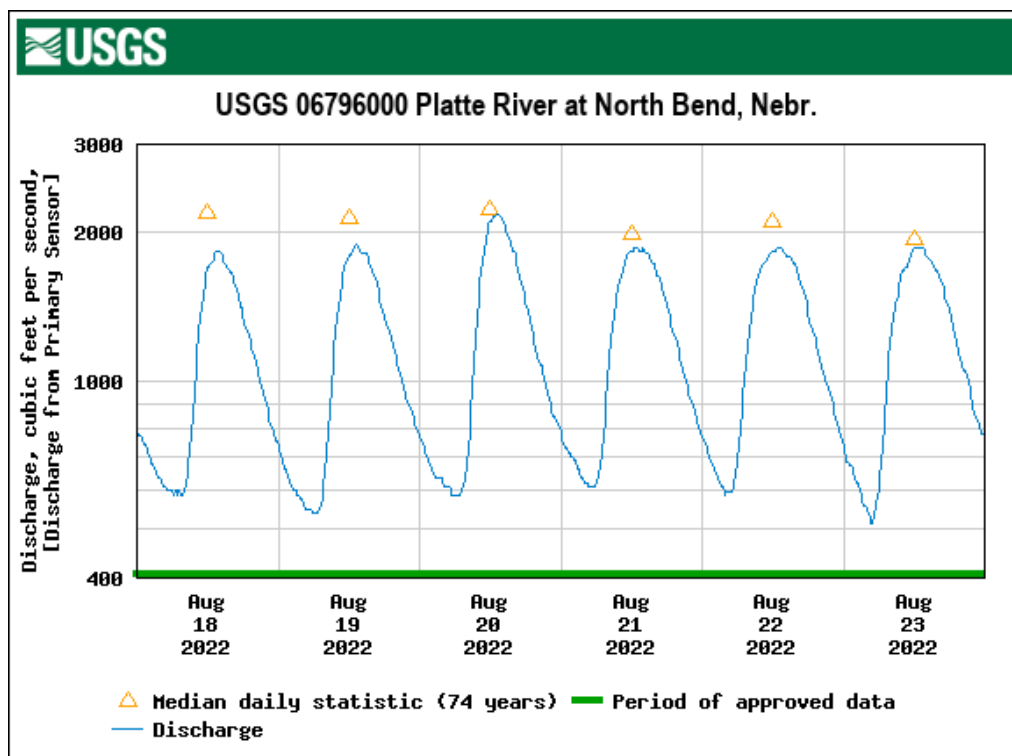


Figure 3: USGS Station 06796000 gage height along the Platte River at the time of lidar acquisition.



Figure 4: These photos, taken by NV5 acquisition staff, display water clarity conditions within the Lower Platte River site.

Airborne Lidar Survey

The lidar survey was accomplished using a Riegl VQ-880-GII green laser system mounted in a Cessna Caravan. The Riegl VQ-880-GII boasts a higher repetition pulse rate (up to 550 kHz), higher scanning speed, small laser footprint, and wide field of view which allows for seamless collection of high resolution data of both topographic and bathymetric surfaces. The green wavelength ($\lambda=532$ nm) laser is capable of collecting high resolution topography data, as well as penetrating the water surface with minimal spectral absorption by water. The Riegl VQ-880-GII contains an integrated NIR laser ($\lambda=1064$ nm) that adds additional topography data and aids in water surface modeling. The Riegl VQ-880-GII laser system can record unlimited range measurements (returns) per pulse, however a maximum of 15 returns can be stored due to LAS v1.4 file limitations. The recorded waveform enables range measurements for all discernible targets for a given pulse. The typical number of returns digitized from a single pulse range from 1 to 14 for the NIR sensor and 1 to 13 for the green sensor in the Lower Platte River project dataset. It is not uncommon for some types of surfaces (e.g., dense vegetation or water) to return fewer pulses to the lidar sensor than the laser originally emitted. The discrepancy between first return and overall delivered density will vary depending on terrain, land cover, and the prevalence of water bodies. All discernible laser returns were processed for the output dataset. Table 5 summarizes the settings used to yield an average pulse density of ≥ 6 pulses/m² over the Lower Platte River project area. Figure 5 shows the flightlines acquired using these lidar specifications.

Table 5: Lidar specifications and survey settings

Parameter	Green Laser	NIR Laser
Acquisition Dates	8/17/2022 - 8/23/2022	8/17/2022 - 8/23/2022
Aircraft Used	Cessna Caravan	Cessna Caravan
Sensor	Riegl	Riegl
Laser	VQ-880GII-Green	VQ-880GII-IR
Maximum Returns	13	14
Resolution/Density	Average 6 pulses/m ²	Average 6 pulses/m ²
Nominal Pulse Spacing	0.41 m	0.41 m
Survey Altitude (AGL)	450 m	450 m
Survey speed	145 knots	145 knots
Field of View	40°	42°
Mirror Scan Rate	80 Lines per Second	Uniform Point Spacing
Target Pulse Rate	200 kHz	300 kHz
Pulse Length	1.5 ns	3 ns
Laser Pulse Footprint Diameter	31.5 cm	9 cm
Central Wavelength	532 nm	1064 nm
Pulse Mode	Multiple Times Around	Multiple Times Around
Beam Divergence	0.7 mrad	0.2 mrad
Swath Width	328 m	345 m
Swath Overlap	60%	60%
Intensity	16-bit	16-bit
Vertical Accuracy	RMSE _Z ≤ 9.2 cm	RMSE _Z ≤ 9.2 cm
Horizontal Accuracy	RMSE _{NE} ≤ 60 cm	RMSE _{NE} ≤ 60 cm

All areas were surveyed with an opposing flight line side-lap of $\geq 50\%$ ($\geq 100\%$ overlap) in order to reduce laser shadowing and increase surface laser painting. To accurately solve for laser point position (geographic coordinates x, y and z), the positional coordinates of the airborne sensor and the orientation of the aircraft to the horizon (attitude) were recorded continuously throughout the lidar data collection mission. Position of the aircraft was measured twice per second (2 Hz) by an onboard differential GPS unit, and aircraft attitude was measured 200 times per second (200 Hz) as pitch, roll and yaw (heading) from an onboard inertial measurement unit (IMU). To allow for post-processing correction and calibration, aircraft and sensor position and attitude data are indexed by GPS time.

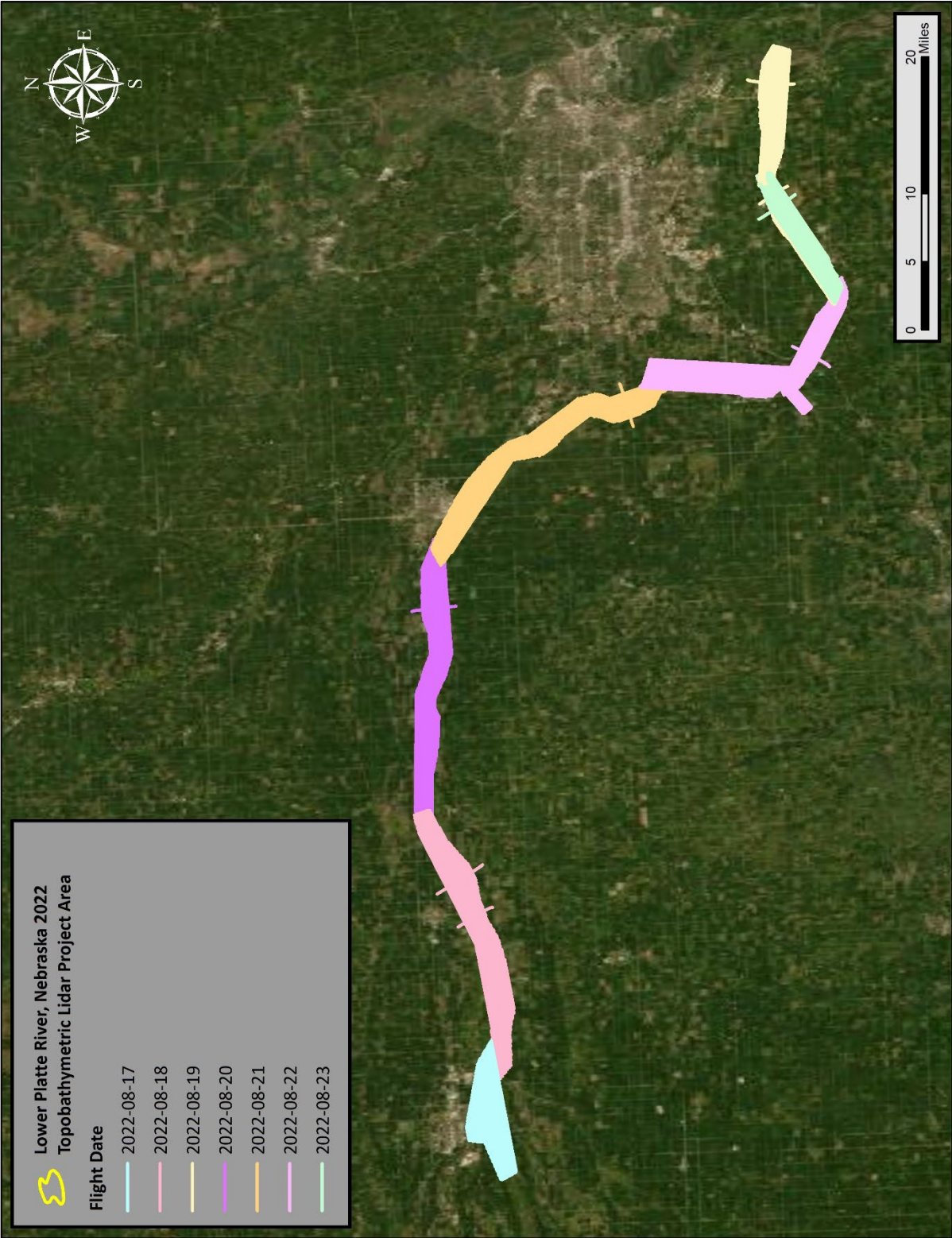


Figure 5: Flightlines map

Ground Survey

Ground control surveys, including ground survey points (GSPs), were conducted to support the airborne acquisition. Ground control data were used to geospatially correct the aircraft positional coordinate data and to perform quality assurance checks on final lidar data.

Base Stations

Monuments were used for collection of ground survey points using real time kinematic (RTK) survey techniques.

Base station locations were selected with consideration for satellite visibility, field crew safety, and optimal location for GSP coverage. NV5 utilized four real time network (RTN) base stations, two from the Hexagon SmartNet network and two from Trimble VRS Now for the Lower Platte River Lidar project (Table 6, Figure 6). NV5's professional land surveyor, Steven J. Hyde (NEPLS#769) oversaw and certified the ground survey.

Table 6: Base station positions for the Lower Platte River acquisition. Coordinates are on the NAD83 (2011) datum, epoch 2010.00

Monument ID	Latitude	Longitude	Ellipsoid (meters)	Network
NECO	41° 25' 47.28732"	-97° 21' 49.64491"	425.871	SMARTNET
NEFM	41° 27' 03.33493"	-96° 32' 15.37125"	348.862	SMARTNET
NEOA	41° 09' 02.71143"	-96° 09' 38.80531"	337.978	TRIMBLE VRS NOW
NESW	40° 52' 06.74479"	-97° 06' 09.18615"	437.928	TRIMBLE VRS NOW

NV5 Geospatial utilized static Global Navigation Satellite System (GNSS) data collected at 1 Hz recording frequency for each base station. During post-processing, the static GNSS data was triangulated with nearby Continuously Operating Reference Stations (CORS) using the Online Positioning User Service (OPUS¹) for precise positioning. Multiple independent sessions over the same monument were processed to confirm antenna height measurements and to refine position accuracy.

Ground Survey Points (GSPs)

Ground survey points were collected using real time kinematic (RTK). For RTK surveys, a roving receiver receives corrections from a nearby base station or Real-Time Network (RTN) via radio or cellular network, enabling rapid collection of points with relative errors less than 1.5 cm horizontal and 2.0 cm vertical. RTK surveys record data while stationary for at least five seconds, calculating the position using at least three one-second epochs. All GSP measurements were made during periods with a Position

¹ OPUS is a free service provided by the National Geodetic Survey to process corrected monument positions: [OPUS website](https://www.ngs.noaa.gov/OPUS/)

Dilution of Precision (PDOP) of ≤ 3.0 with at least six satellites in view of the stationary and roving receivers. See Table 7 for NV5 ground survey equipment information.

GSPs were collected in areas where good satellite visibility was achieved on paved roads and other hard surfaces such as gravel roads. GSP measurements were not taken on highly reflective surfaces such as center line stripes or lane markings on roads due to the increased noise seen in the laser returns over these surfaces. GSPs were collected within as many flightlines as possible; however, the distribution of GSPs depended on ground access constraints and monument locations and may not be equably distributed throughout the study area (Figure 6).

Table 7: NV5 Geospatial ground survey equipment identification

Receiver Model	Antenna	OPUS Antenna ID	Use
Trimble R12	Integrated Antenna	TRMR12	Rover

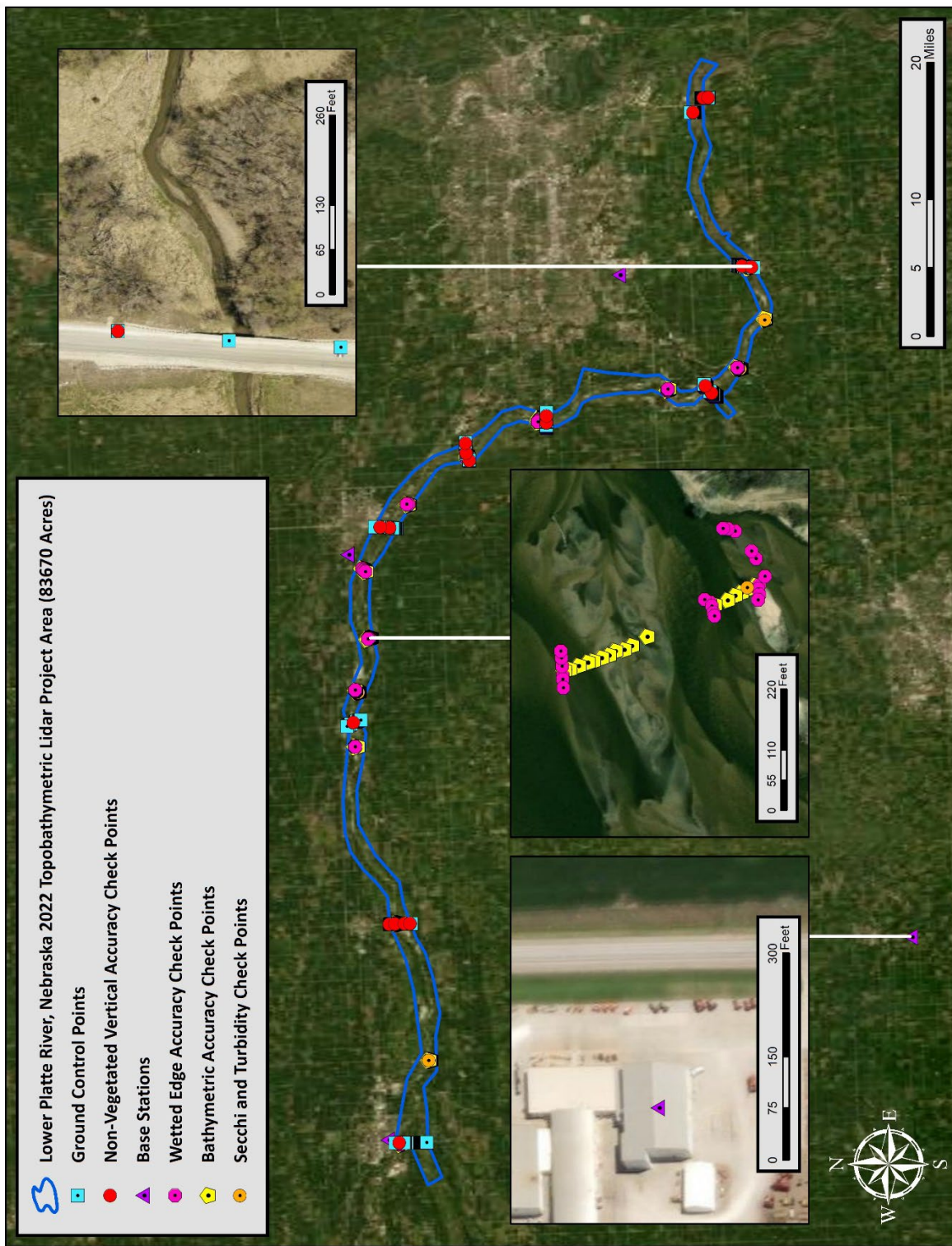


Figure 6: Ground survey location map

PROCESSING

- Ground
- Default
- Water Surface
- Bathymetric Bottom

This 3 foot lidar cross section shows a view of the Lower Platte River landscape, colored by point classification.

Topobathymetric Lidar Data

Upon completion of data acquisition, NV5 processing staff initiated a suite of automated and manual techniques to process the data into the requested deliverables. Processing tasks included GPS control computations, smoothed best estimate trajectory (SBET) calculations, kinematic corrections, calculation of laser point position, sensor and data calibration for optimal relative and absolute accuracy, and lidar point classification (Table 8).

Riegl's RiProcess software was used to facilitate bathymetric return processing. Once bathymetric points were differentiated, they were spatially corrected for refraction through the water column based on the angle of incidence of the laser. NV5 refracted water column points using NV5's proprietary LAS processing software, Las Monkey. The resulting point cloud data was classified using both manual and automated techniques. Processing methodologies were tailored for the landscape. Brief descriptions of these tasks are shown in Table 9.

Table 8: ASPRS LAS classification standards applied to the Lower Platte River dataset

Classification Number	Classification Name	Classification Description
1	Default/Unclassified	Laser returns that are not included in the ground class, composed of vegetation and anthropogenic features
1-0	Overlap	Laser returns at the outer edges of flightlines that are geometrically unreliable
2	Ground	Laser returns that are determined to be ground using automated and manual cleaning algorithms
7	Noise	Laser returns that are often associated with birds, scattering from reflective surfaces, or artificial points below the ground surface
9	Water	Laser returns that are determined to be water using automated and manual cleaning algorithms
40	Bathymetric Bottom	Refracted green laser returns that fall within the water's edge breakline which characterize the submerged topography.
41	Water Surface	Green laser returns that are determined to be water surface points using automated and manual cleaning algorithms.
45	Water Column	Refracted green sensor returns that are determined to be water using automated and manual cleaning algorithms.

Table 9: Lidar processing workflow

Lidar Processing Step	Software Used
Resolve kinematic corrections for aircraft position data using kinematic aircraft GPS and static ground GPS data. Develop a smoothed best estimate of trajectory (SBET) file that blends post-processed aircraft position with sensor head position and attitude recorded throughout the survey.	POSPac MMS v.8.7
Calculate laser point position by associating SBET position to each laser point return time, scan angle, intensity, etc. Create raw laser point cloud data for the entire survey in *.las (ASPRS v. 1.4) format. Convert data to orthometric elevations by applying a geoid correction.	RiUnite v1.0.3
Import raw laser points into manageable blocks (less than 500 MB) to perform manual relative accuracy calibration and filter erroneous points. Classify ground points for individual flight lines.	TerraScan v.19.005
Using ground classified points per each flight line, test the relative accuracy. Perform automated line-to-line calibrations for system attitude parameters (pitch, roll, heading), mirror flex (scale) and GPS/IMU drift. Calculate calibrations on ground classified points from paired flight lines and apply results to all points in a flight line. Use every flight line for relative accuracy calibration.	StripAlign v.2.2.1
Apply refraction correction to all subsurface returns.	Las Monkey v.2.6.6 (NV5 Geospatial proprietary)
Classify resulting data to ground and other client designated ASPRS classifications (Table 8). Assess statistical absolute accuracy via direct comparisons of ground classified points to ground control survey data.	TerraScan v.19.005 TerraModeler v.19.003
Generate bare earth models as triangulated surfaces. Generate highest hit models as a surface expression of all classified points. Export all surface models as ERDAS Imagine (.img) format at a 3.0 foot pixel resolution.	Las Product Creator 4.0 (NV5 proprietary software) ArcMap v. 10.8
Export intensity images as cloud optimized GeoTIFFs at a 1.5 foot pixel resolution.	Las Monkey v.2.6.6 (NV5 Geospatial proprietary) ArcMap v. 10.8 Las Product Creator 4.0 (NV5 proprietary software)

Bathymetric Refraction

Green lidar pulses that enter the water column must have their position corrected for refraction of the light beam as it passes through the water and its resulting decreased speed. NV5 has developed proprietary software (Las Monkey) to perform this processing based on Snell's law. The first step is to develop a water surface model (WSM) covering all submerged returns within the project boundary. The water surface model used for refraction is generated from points within the wetted edge breaklines that include NIR points representing the water surface as well as elevations sampled from the ground at the water's edge. Points are filtered and edited to obtain the most accurate representation of the water surface and are used to create a water surface model TIN. A TIN model is preferable to a raster based water surface model in obtaining the most accurate angle of incidence during refraction.

Once the WSM is generated, the Las Monkey refraction software then intersects the partially submerged green pulses with the WSM to determine the angle of incidence with the water surface and the submerged component of the pulse vector. This provides the information necessary to correct the position of underwater points by adjusting the submerged vector length and orientation. After refraction, the points are compared against bathymetric check points to assess accuracy.

Lidar Derived Products

Because hydrographic laser scanners penetrate the water surface to map submerged topography, this affects how the data should be processed and presented in derived products from the lidar point cloud. The following section discusses certain derived products that vary from the traditional (NIR) specification and delivery format.

Topobathymetric DEMs

Bathymetric bottom returns can be limited by depth, water clarity, and bottom surface reflectivity. Water clarity and turbidity affects the depth penetration capability of the green wavelength laser with returning laser energy diminishing by scattering throughout the water column. Additionally, the bottom surface must be reflective enough to return remaining laser energy back to the sensor at a detectable level. Although the predicted depth penetration range of the Riegl VQ-880-GII sensor is 1.5 Secchi depths on brightly reflective surfaces, it is not unexpected to have no bathymetric bottom returns in turbid or non-reflective areas.

As a result, creating digital elevation models (DEMs) presents a challenge with respect to interpolation of areas with no returns. Traditional DEMs are "unclipped", meaning areas lacking ground returns are interpolated from neighboring ground returns (or breaklines in the case of hydro-flattening), with the assumption that the interpolation is close to reality. In bathymetric modeling, these assumptions are prone to error because a lack of bathymetric returns can indicate a change in elevation that the laser can no longer map due to increased depths. The resulting void areas may suggest greater depths, rather than similar elevations from neighboring bathymetric bottom returns. Therefore, NV5 created a water polygon with bathymetric coverage to delineate areas with successfully mapped bathymetry. This shapefile was used to control the extent of the delivered clipped topobathymetric model to avoid false triangulation (interpolation from TIN'ing) across areas in the water without bathymetric bottom returns.

Intensity Images

The first returns of all valid point classes were used for both the green and NIR sensors in order to create intensity images. With bathymetric lidar a more detailed and informative intensity image can be created by using all or selected point classes, rather than relying on return number alone. If intensity information of the bathymetry is the primary goal, water surface and water column points can be excluded. However, water surface and water column points often contain potentially useful information about turbidity and submerged but unclassified features such as vegetation. For the Lower Platte River project, NV5 created one set of intensity images from NIR laser first returns, as well as one set of intensity images from green laser returns (Figure 7).

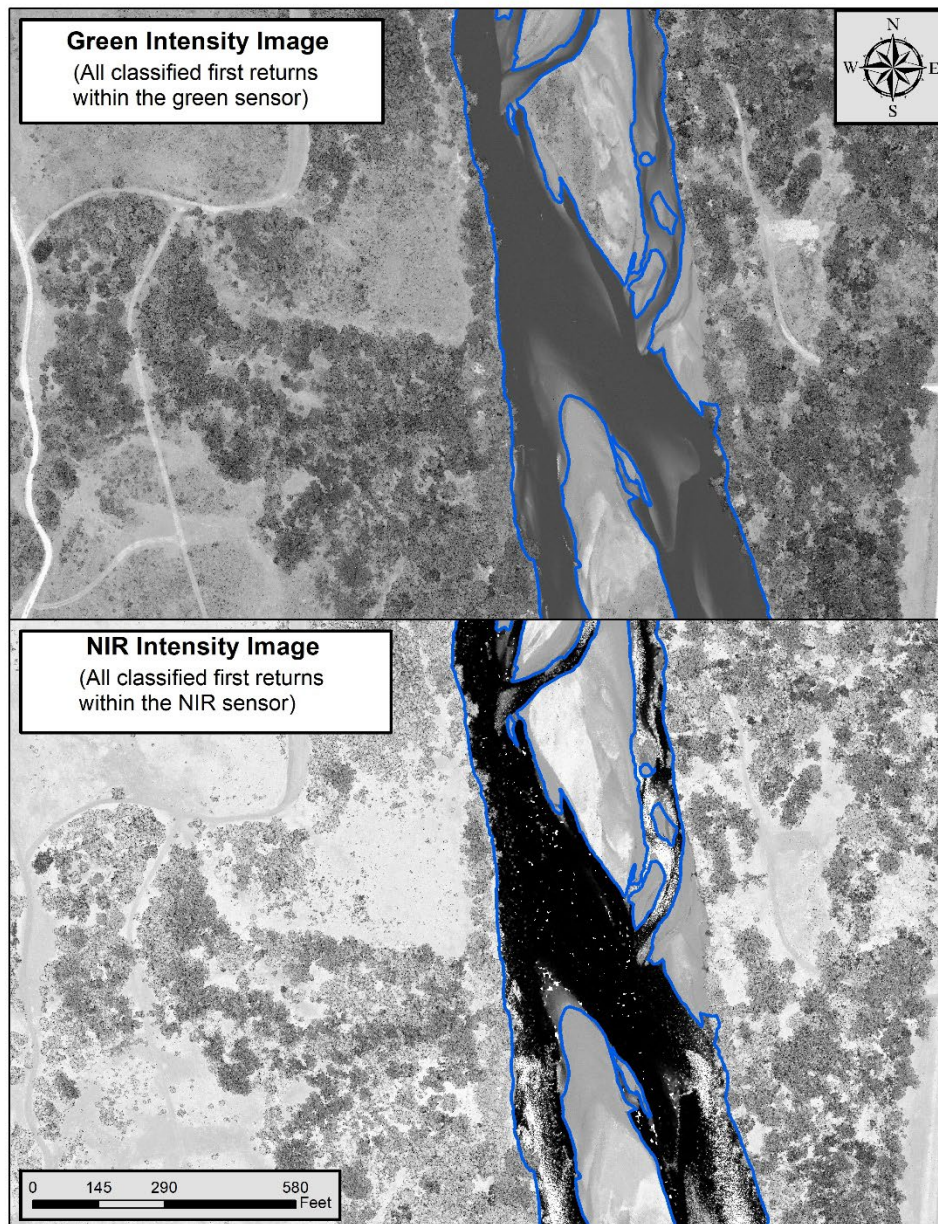


Figure 7: A comparison of Intensity Images from Green and NIR first returns in the Lower Platte River area

Feature Extraction

Hydroflattening and Water's edge breaklines

The Lower Platte River and other water bodies within the project area were flattened to a consistent water level. Bodies of water that were flattened include lakes and other closed water bodies with a surface area greater than 2 acres. The hydroflattening process eliminates artifacts in the digital terrain model caused by both increased variability in ranges or dropouts in laser returns due to the low reflectivity of water.

Hydroflattening of closed water bodies was performed through a combination of automated and manual detection and adjustment techniques designed to identify water boundaries and water levels. Boundary polygons were developed using an algorithm which weights lidar-derived slopes, intensities, and return densities to detect the water's edge. The water edges were then manually reviewed and edited as necessary.

Once polygons were developed the initial ground classified points falling within water polygons were reclassified as water points to omit them from the final ground model. Elevations were then obtained from the filtered lidar returns to create the final breaklines. Lakes were assigned a consistent elevation for an entire polygon while rivers were assigned consistent elevations on opposing banks and smoothed to ensure downstream flow through the entire river channel.

Water boundary breaklines were then incorporated into the hydroflattened DEM by enforcing triangle edges (adjacent to the breakline) to the elevation values of the breakline. This implementation corrected interpolation along the hard edge. Water surfaces were obtained from a TIN of the 3-D water edge breaklines resulting in the final hydroflattened model (Figure 8).

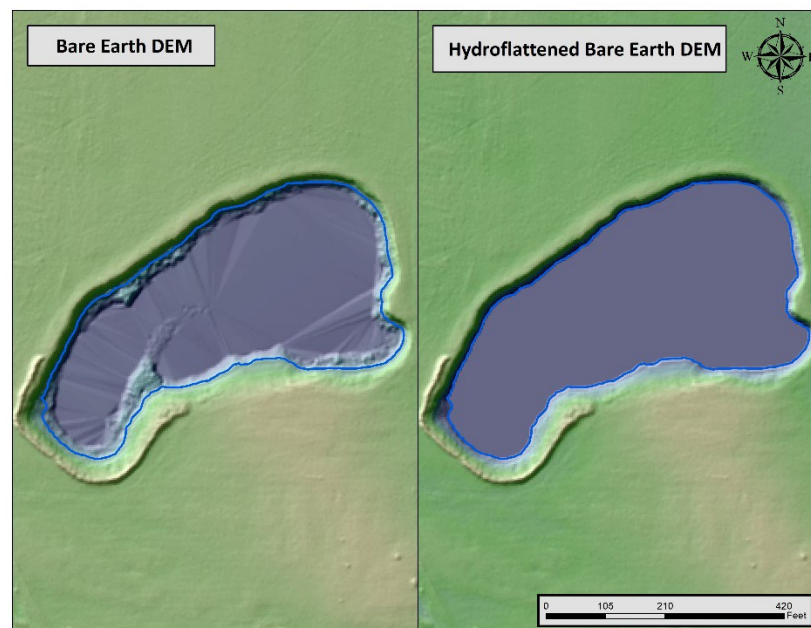
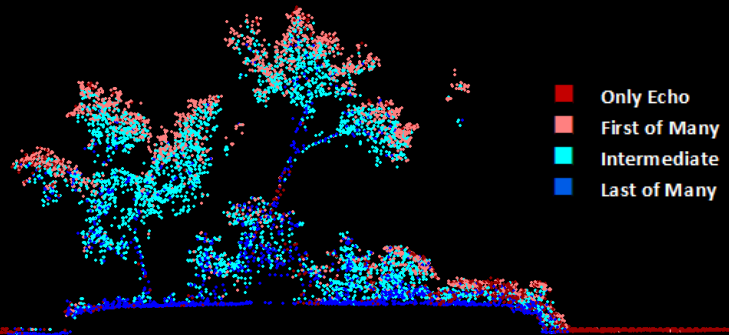


Figure 8: Example of hydroflattening in the Lower Platte River dataset

This 3 foot LiDAR cross section shows a view of an island on the river in the Lower Platte AOI, colored by point laser echo.



Bathymetric Lidar

An underlying principle for collecting hydrographic lidar data is to survey near-shore areas that can be difficult to collect with other methods, such as multi-beam sonar, particularly over large areas. The capability and effectiveness of the bathymetric lidar is impacted by several parameters including depth penetrations below the water surface, bathymetric return density, and spatial accuracy.

Mapped Bathymetry and Depth Penetration

The specified depth penetration range of the Riegl VQ-880-GII sensor is 1.5 secchi depths; therefore, bathymetry data below one secchi depth at the time of acquisition is not to be expected. To assist in evaluating performance results of the sensor, a polygon layer was created to delineate areas where bathymetry was successfully mapped.

This shapefile was used to control the extent of the delivered clipped topo-bathymetric model and to avoid false triangulation across areas in the water with no returns. Insufficiently mapped areas were identified by triangulating bathymetric bottom points with an edge length maximum of 15.2 feet. This ensured all areas of no returns ($> 96.88 \text{ ft}^2$), were identified as data voids. Overall NV5 Geospatial successfully mapped 47.19% of the bathymetric areas in the Lower Platte River AOI. Of the areas successfully mapped, 98.2% had a calculated depth of 0 - 2 feet, 1.4% had a calculated depth of 2 - 4 feet, 0.33% had a calculated depth of 4 - 6 feet, 0.12% had a calculated depth of 6 - 8 feet, 0.05% had a calculated depth of 8 - 10 feet, and the remaining 0.02% had a calculated depth greater than 10 feet (Figure 9). The maximum recorded depth for the Lower Platte River topobathymetric dataset was 14.6 feet.

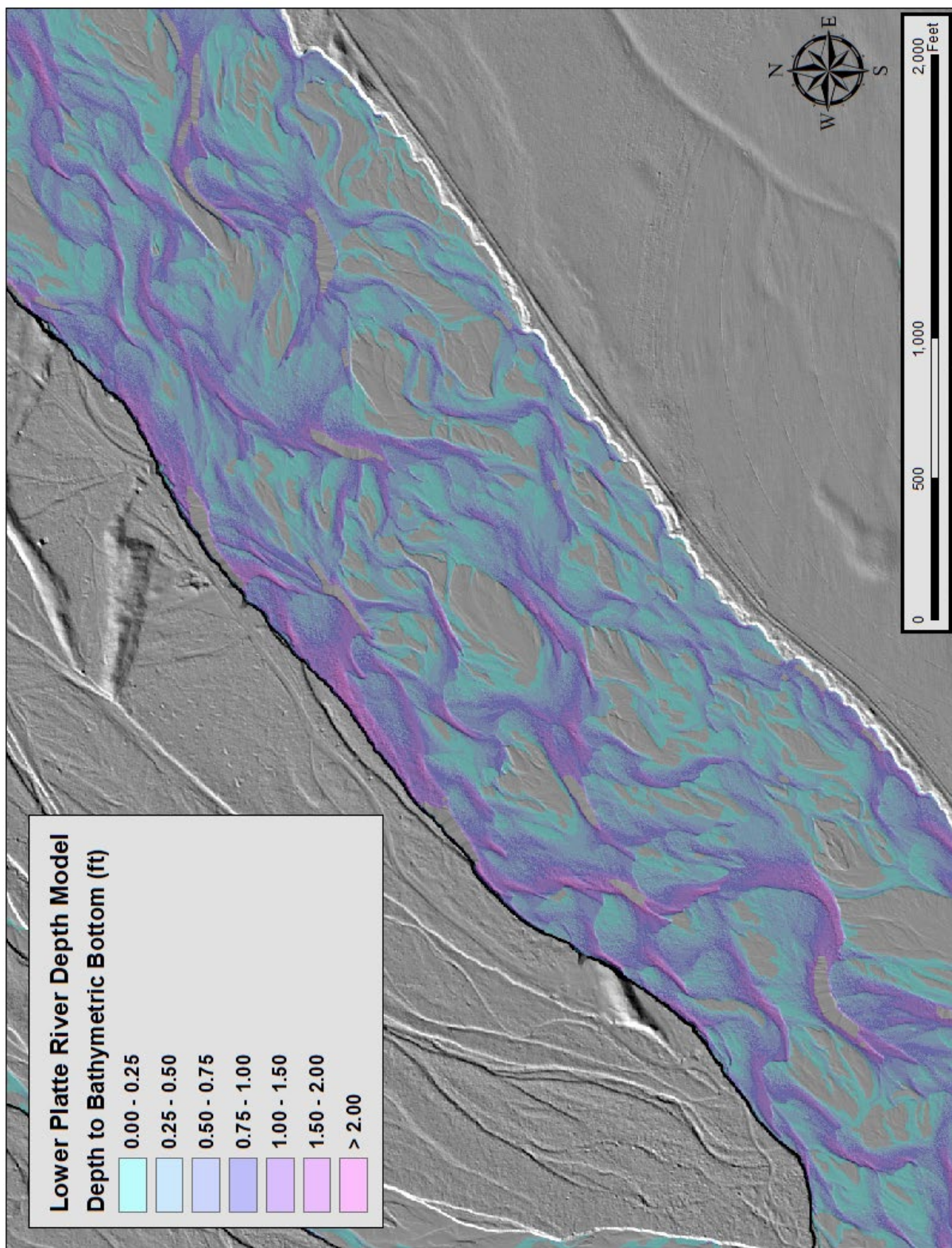


Figure 9: Depth model of the Skagit River

Lidar Point Density

First Return Point Density

The acquisition parameters were designed to acquire an average first-return density of 6 points/m² (0.56 points/ft²). First return density describes the density of pulses emitted from the laser that return at least one echo to the system. Multiple returns from a single pulse were not considered in first return density analysis. Some types of surfaces (e.g., breaks in terrain, water and steep slopes) may have returned fewer pulses than originally emitted by the laser.

First returns typically reflect off the highest feature on the landscape within the footprint of the pulse. In forested or urban areas the highest feature could be a tree, building or power line, while in areas of unobstructed ground, the first return will be the only echo and represents the bare earth surface.

The average first-return density of the Lower Platte River Lidar project was 2.93 points/ft² (31.52 points/m²) (Table 10). The statistical and spatial distributions of all first return densities per 100 m x 100 m cell are portrayed in Figure 10 and Figure 17.

Bathymetric and Ground Classified Point Densities

The density of ground classified lidar returns and bathymetric bottom returns were also analyzed for this project. Terrain character, land cover, and ground surface reflectivity all influenced the density of ground surface returns. In vegetated areas, fewer pulses may have penetrated the canopy, resulting in lower ground density. Similarly, the density of bathymetric bottom returns was influenced by turbidity, depth, and bottom surface reflectivity. In turbid areas, fewer pulses may have penetrated the water surface, resulting in lower bathymetric density.

The ground and bathymetric bottom classified density of lidar data for the Lower Platte River project was 0.89 points/ft² (9.57 points/m²)(Table 10). The statistical and spatial distributions per 100 m x 100 m cell of the ground and bathymetric bottom classified return densities are portrayed in Figure 11 and Figure 17.

Additionally, for the Lower Platte River project, density values of only bathymetric bottom returns were calculated for areas containing at least one bathymetric bottom return. Areas lacking bathymetric returns (voids) were not considered in calculating an average density value. Within the successfully mapped area, a bathymetric bottom return density of 1.13 points/ft² (12.19 points/m²) was achieved.

Table 10: Average Lidar point densities

Density Type	Point Density
First Returns	2.93 points/ft ²
	31.52 points/m ²
Ground and Bathymetric Bottom Classified Returns	0.89 points/ft ²
	9.57 points/m ²
Bathymetric Bottom Classified Returns	1.13 points/ft ²
	12.19 points/m ²

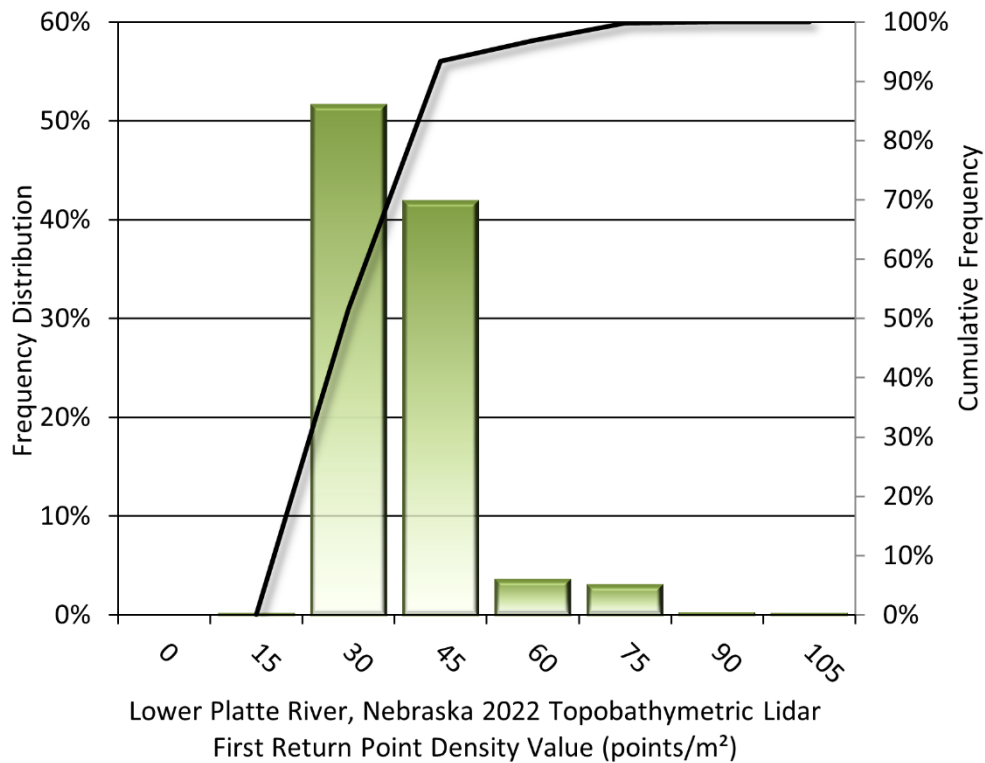


Figure 10: Frequency distribution of first return densities per 100 x 100 m cell

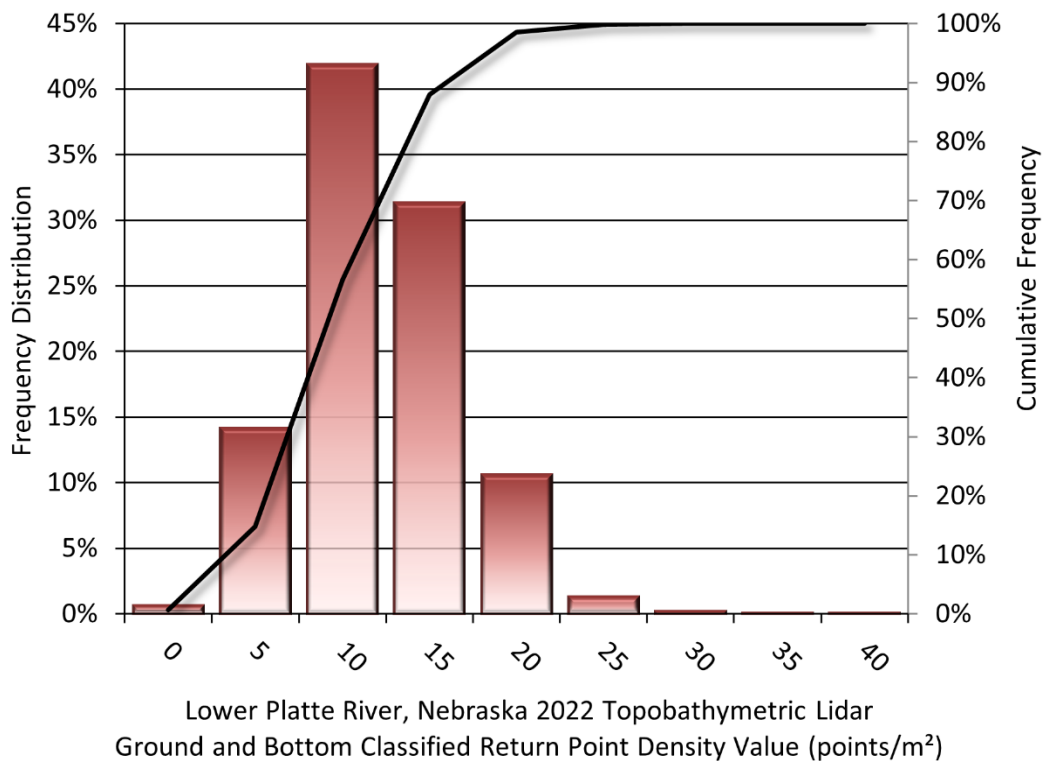


Figure 11: Frequency distribution of ground and bathymetric bottom classified return densities per 100 x 100 m cell

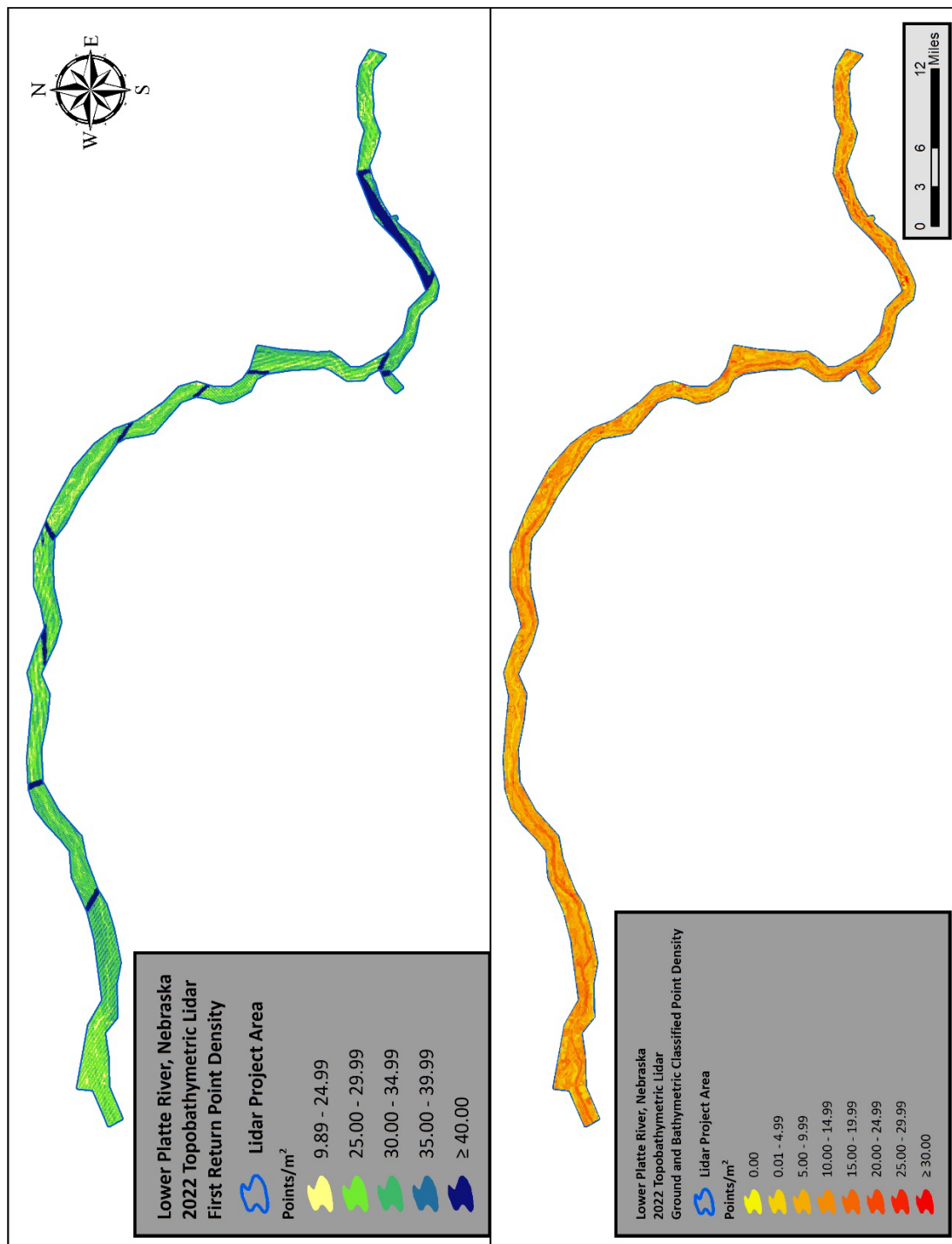


Figure 12: First return and ground and bathymetric bottom density map for the Lower Platte River site (100 m x 100 m cells)

Lidar Accuracy Assessments

The accuracy of the lidar data collection can be described in terms of absolute accuracy (the consistency of the data with external data sources) and relative accuracy (the consistency of the dataset with itself). See Appendix A for further information on sources of error and operational measures used to improve relative accuracy.

Lidar Non-Vegetated Vertical Accuracy

Absolute accuracy was assessed using Non-vegetated Vertical Accuracy (NVA) reporting designed to meet guidelines presented in the FGDC National Standard for Spatial Data Accuracy². NVA compares known ground check point data that were withheld from the calibration and post-processing of the lidar point cloud to the triangulated surface generated by the classified lidar point cloud as well as the derived gridded bare earth DEM. NVA is a measure of the accuracy of lidar point data in open areas where the lidar system has a high probability of measuring the ground surface and is evaluated at the 95% confidence interval ($1.96 * RMSE$), as shown in Table 11.

The mean and standard deviation (σ) of divergence of the ground surface model from ground check point coordinates are also considered during accuracy assessment. These statistics assume the error for x, y and z is normally distributed, and therefore the skew and kurtosis of distributions are also considered when evaluating error statistics. For the Lower Platte River survey, 16 ground check points were withheld from the calibration and post-processing of the lidar point cloud, with resulting non-vegetated vertical accuracy of 0.181 feet (0.055 meters), as compared to the classified LAS and 0.206 feet (0.063 meters) against the bare earth DEM, with 95% confidence (Figure 13 and Figure 14).

NV5 also assessed absolute accuracy using 384 ground control points. Although these points were used in the calibration and post-processing of the lidar point cloud, they still provide a good indication of the overall accuracy of the lidar dataset, and therefore have been provided in Table 11 and Figure 15.

Table 11: Absolute accuracy results

Parameter	NVA, as compared to Classified LAS	NVA, as compared to Bare Earth DEM	Ground Control Points
Sample	16 points	16 points	384 points
95% Confidence ($1.96 * RMSE$)	0.181 ft 0.055 m	0.206 ft 0.063 m	0.153 ft 0.047 m
Average	-0.027 ft -0.008 m	-0.029 ft -0.009 m	-0.004 ft -0.001 m
Median	-0.033 ft -0.010 m	-0.031 ft -0.010 m	-0.010 ft -0.003 m
RMSE	0.092 ft 0.028 m	0.105 ft 0.032 m	0.078 ft 0.024 m
Standard Deviation (1σ)	0.091 ft 0.028 m	0.104 ft 0.032 m	0.078 ft 0.024 m

² Federal Geographic Data Committee, ASPRS POSITIONAL ACCURACY STANDARDS FOR DIGITAL GEOSPATIAL DATA EDITION 1, Version 1.0, NOVEMBER 2014.
https://www.asprs.org/a/society/committees/standards/Positional_Accuracy_Standards.pdf.

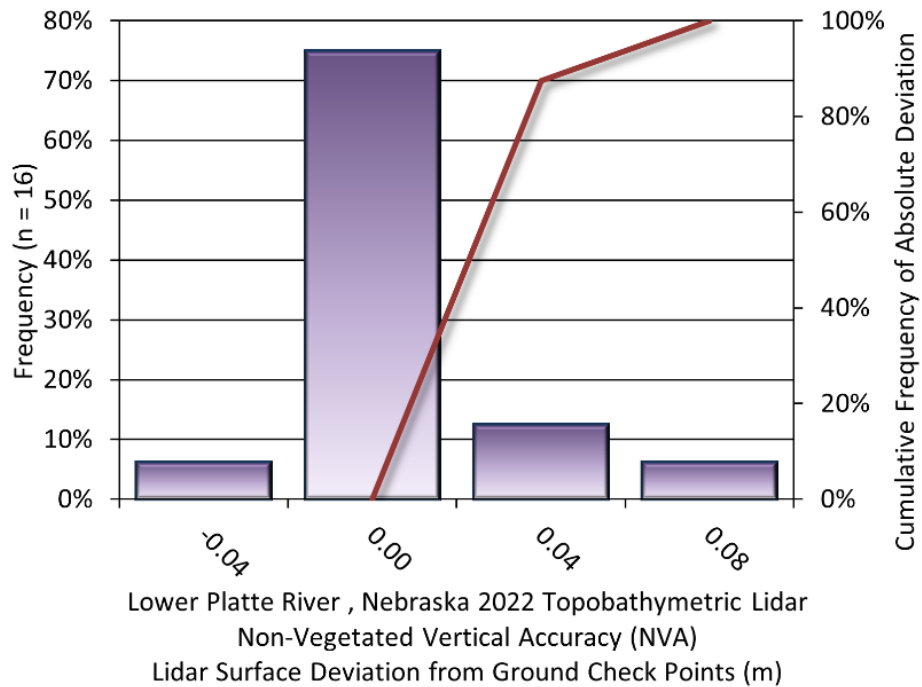


Figure 13: Frequency histogram for classified LAS deviation from ground check point values

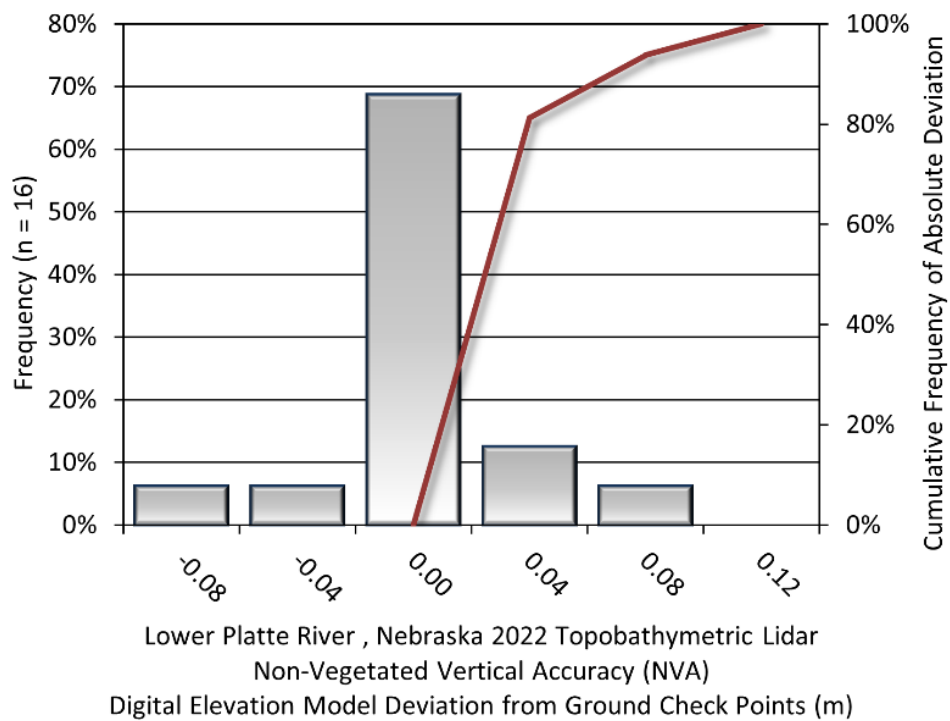


Figure 14: Frequency histogram for lidar bare earth DEM deviation from ground check point values

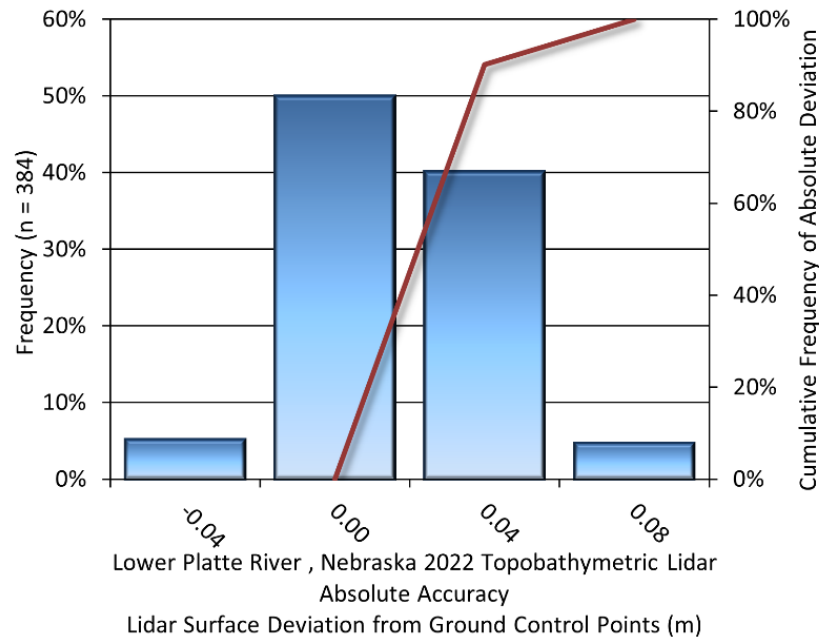


Figure 15: Frequency histogram for lidar surface deviation ground control point values

Lidar Bathymetric Vertical Accuracies

Bathymetric (submerged or along the water's edge) check points were also collected in order to assess the submerged surface vertical accuracy. Assessment of 637 submerged bathymetric check points resulted in a vertical accuracy of 0.372 feet (0.113 meters), while assessment of 289 wetted edge check points resulted in a vertical accuracy of 0.344 feet (0.105 meters), evaluated at 95% confidence interval (Table 12, Figure 16, and Figure 17).

Table 12: Bathymetric Vertical Accuracy for the Lower Platte River Project

Parameter	Submerged Bathymetric Check Points	Wetted Edge Bathymetric Check Points
Sample	637 points	289 points
95% Confidence (1.96*RMSE)	0.372 ft 0.113 m	0.344 ft 0.105 m
Average Dz	-0.075 ft -0.023 m	-0.092 ft -0.028 m
Median	-0.095 ft -0.029 m	-0.075 ft -0.023 m
RMSE	0.190 ft 0.058 m	0.176 ft 0.054 m
Standard Deviation (1σ)	0.174 ft 0.053 m	0.150 ft 0.046 m

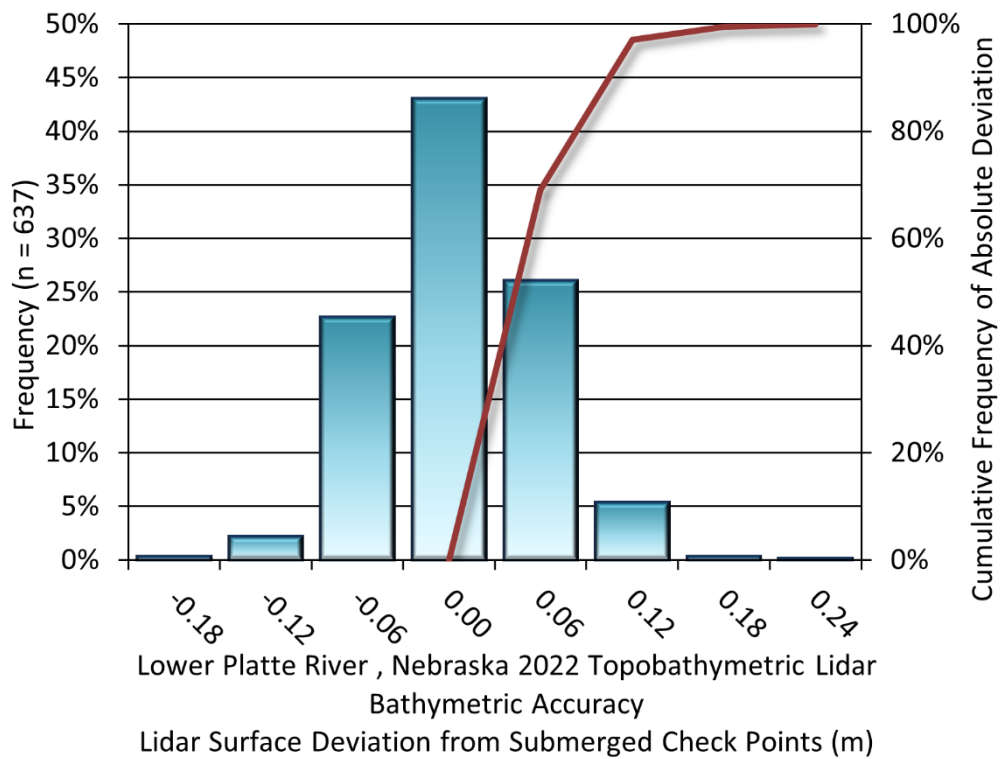


Figure 16: Frequency histogram for lidar surface deviation from submerged check point values

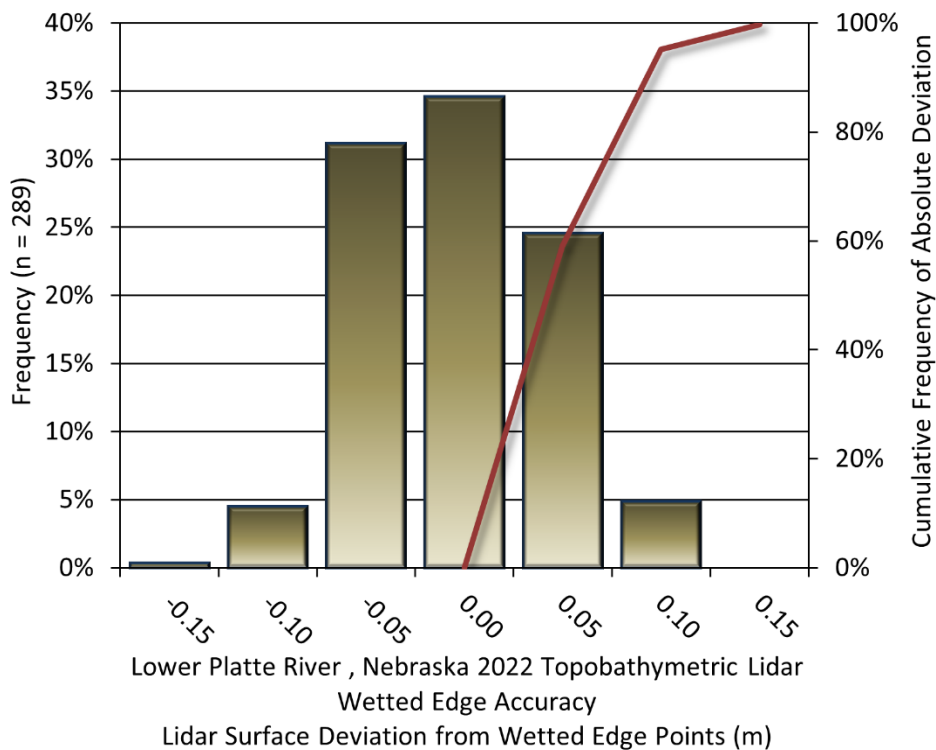


Figure 17: Frequency histogram for lidar surface deviation from wetted edge check point values

Lidar Relative Vertical Accuracy

Relative vertical accuracy refers to the internal consistency of the data set as a whole: the ability to place an object in the same location given multiple flight lines, GPS conditions, and aircraft attitudes. When the lidar system is well calibrated, the swath-to-swath vertical divergence is low (<0.10 meters). The relative vertical accuracy was computed by comparing the ground surface model of each individual flight line with its neighbors in overlapping regions. The average (mean) line to line relative vertical accuracy for the Lower Platte River Lidar project was 0.096 feet (0.029 meters) (Table 13, Figure 18).

Table 13: Relative accuracy results

Parameter	Relative Accuracy
Sample	700 flight line surfaces
Average	0.096 ft 0.029 m
Median	0.093 ft 0.028 m
RMSE	0.097 ft 0.030 m
Standard Deviation (1 σ)	0.018 ft 0.005 m
1.96 σ	0.035 ft 0.011 m

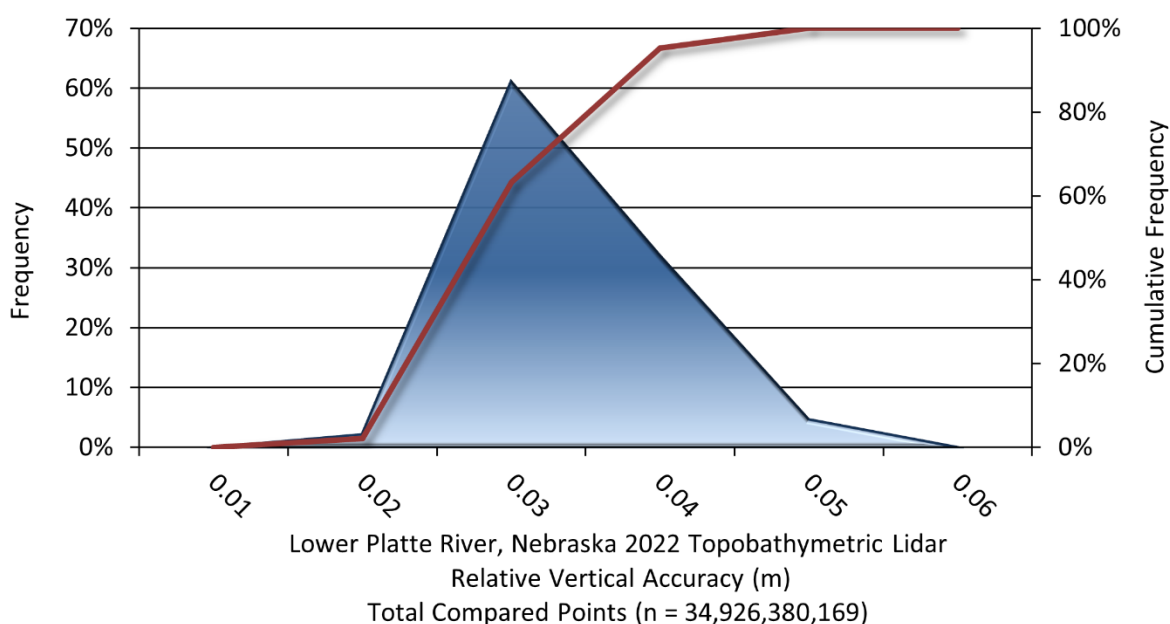


Figure 18: Frequency plot for relative vertical accuracy between flight lines

Lidar Horizontal Accuracy

Lidar horizontal accuracy is a function of Global Navigation Satellite System (GNSS) derived positional error, flying altitude, and inertial navigation system (INS) derived attitude error. The obtained $RMSE_r$ value is multiplied by a conversion factor of 1.7308 to yield the horizontal component of the National Standards for Spatial Data Accuracy (NSSDA) reporting standard where a theoretical point will fall within the obtained radius 95 percent of the time. Based on a flying altitude of 450 meters, an IMU error of 0.002 decimal degrees, and a GNSS positional error of 0.023 meters, this project was produced to meet 0.655 feet (0.200 m) horizontal accuracy at the 95% confidence level (Table 14).

Table 14: Horizontal Accuracy

Parameter	Horizontal Accuracy
$RMSE_r$	0.119 ft
	0.036 m
ACC_r	0.206 ft
	0.063 m

CERTIFICATIONS

NV5 Geospatial provided lidar services for the Lower Platte River project as described in this report.

I, Steven Miller, have reviewed the attached report for completeness and hereby state that it is a complete and accurate report of this project.


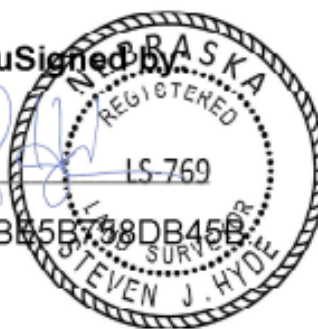


Mar 6, 2023

Steven Miller
Project Manager
NV5 Geospatial

I, Steven J. Hyde, PLS, being duly registered as a Professional Land Surveyor in and by the state of Nebraska hereby certify that the methodologies, static GNSS occupations used during airborne flights, and ground survey point collection were performed using commonly accepted Standard Practices. Field work conducted for this report was conducted between August 18 to August 25th and November 07, 2022.

Accuracy statistics shown in the Accuracy Section of this Report have been reviewed by me and found to meet the “National Standard for Spatial Data Accuracy”.

DocuSigned by:

Steven J. Hyde
PLS # 769
NV5 Geospatial
23CB5B738DB45B

3/6/2023

SELECTED IMAGES

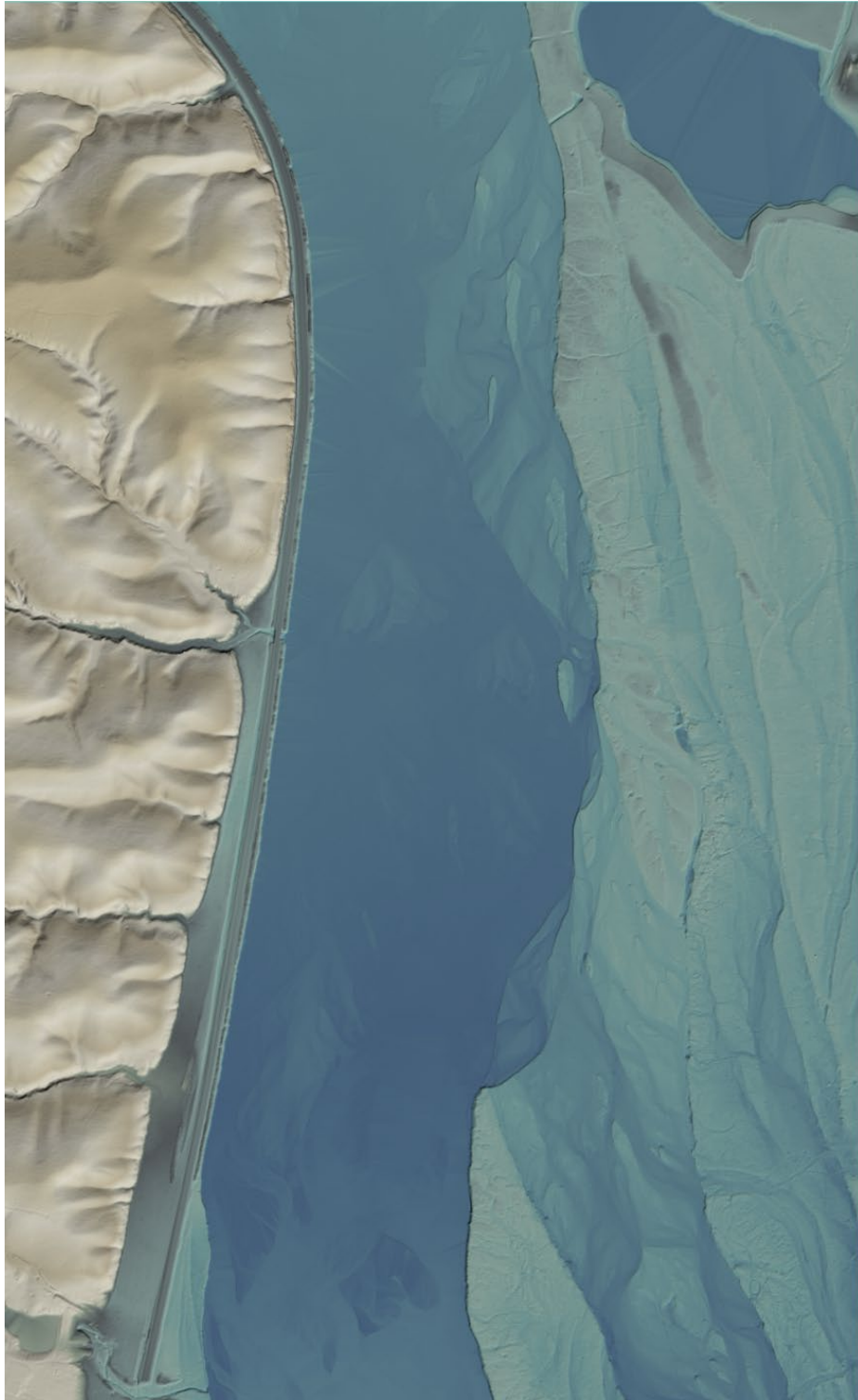


Figure 19: View looking south over Lower Platte River. The image was created from the lidar bare earth model and colored by elevation.

GLOSSARY

1-sigma (σ) Absolute Deviation: Value for which the data are within one standard deviation (approximately 68th percentile) of a normally distributed data set.

1.96 * RMSE Absolute Deviation: Value for which the data are within two standard deviations (approximately 95th percentile) of a normally distributed data set, based on the FGDC standards for Non-vegetated Vertical Accuracy (FVA) reporting.

Accuracy: The statistical comparison between known (surveyed) points and laser points. Typically measured as the standard deviation (sigma σ) and root mean square error (RMSE).

Absolute Accuracy: The vertical accuracy of lidar data is described as the mean and standard deviation (sigma σ) of divergence of lidar point coordinates from ground survey point coordinates. To provide a sense of the model predictive power of the dataset, the root mean square error (RMSE) for vertical accuracy is also provided. These statistics assume the error distributions for x, y and z are normally distributed, and thus we also consider the skew and kurtosis of distributions when evaluating error statistics.

Relative Accuracy: Relative accuracy refers to the internal consistency of the data set; i.e., the ability to place a laser point in the same location over multiple flight lines, GPS conditions and aircraft attitudes. Affected by system attitude offsets, scale and GPS/IMU drift, internal consistency is measured as the divergence between points from different flight lines within an overlapping area. Divergence is most apparent when flight lines are opposing. When the lidar system is well calibrated, the line-to-line divergence is low (<10 cm).

Root Mean Square Error (RMSE): A statistic used to approximate the difference between real-world points and the lidar points. It is calculated by squaring all the values, then taking the average of the squares and taking the square root of the average.

Data Density: A common measure of lidar resolution, measured as points per square meter.

Digital Elevation Model (DEM): File or database made from surveyed points, containing elevation points over a contiguous area. Digital terrain models (DTM) and digital surface models (DSM) are types of DEMs. DTMs consist solely of the bare earth surface (ground points), while DSMs include information about all surfaces, including vegetation and man-made structures.

Intensity Values: The peak power ratio of the laser return to the emitted laser, calculated as a function of surface reflectivity.

Nadir: A single point or locus of points on the surface of the earth directly below a sensor as it progresses along its flight line.

Overlap: The area shared between flight lines, typically measured in percent. 100% overlap is essential to ensure complete coverage and reduce laser shadows.

Pulse Rate (PR): The rate at which laser pulses are emitted from the sensor; typically measured in thousands of pulses per second (kHz).

Pulse Returns: For every laser pulse emitted, the number of wave forms (i.e., echoes) reflected back to the sensor. Portions of the wave form that return first are the highest element in multi-tiered surfaces such as vegetation. Portions of the wave form that return last are the lowest element in multi-tiered surfaces.

Real-Time Kinematic (RTK) Survey: A type of surveying conducted with a GPS base station deployed over a known monument with a radio connection to a GPS rover. Both the base station and rover receive differential GPS data and the baseline correction is solved between the two. This type of ground survey is accurate to 1.5 cm or less.

Post-Processed Kinematic (PPK) Survey: GPS surveying is conducted with a GPS rover collecting concurrently with a GPS base station set up over a known monument. Differential corrections and precisions for the GNSS baselines are computed and applied after the fact during processing. This type of ground survey is accurate to 1.5 cm or less.

Scan Angle: The angle from nadir to the edge of the scan, measured in degrees. Laser point accuracy typically decreases as scan angles increase.

Native Lidar Density: The number of pulses emitted by the lidar system, commonly expressed as pulses per square meter.

APPENDIX A - ACCURACY CONTROLS

Relative Accuracy Calibration Methodology:

Manual System Calibration: Calibration procedures for each mission require solving geometric relationships that relate measured swath-to-swath deviations to misalignments of system attitude parameters. Corrected scale, pitch, roll and heading offsets were calculated and applied to resolve misalignments. The raw divergence between lines was computed after the manual calibration was completed and reported for each survey area.

Automated Attitude Calibration: All data was tested and calibrated using TerraMatch automated sampling routines. Ground points were classified for each individual flight line and used for line-to-line testing. System misalignment offsets (pitch, roll and heading) and scale were solved for each individual mission and applied to respective mission datasets. The data from each mission were then blended when imported together to form the entire area of interest.

Automated Z Calibration: Ground points per line were used to calculate the vertical divergence between lines caused by vertical GPS drift. Automated Z calibration was the final step employed for relative accuracy calibration.

Lidar accuracy error sources and solutions:

Source	Type	Post Processing Solution
Long Base Lines	GPS	None
Poor Satellite Constellation	GPS	None
Poor Antenna Visibility	GPS	Reduce Visibility Mask
Poor System Calibration	System	Recalibrate IMU and sensor offsets/settings
Inaccurate System	System	None
Poor Laser Timing	Laser Noise	None
Poor Laser Reception	Laser Noise	None
Poor Laser Power	Laser Noise	None
Irregular Laser Shape	Laser Noise	None

Operational measures taken to improve relative accuracy:

Focus Laser Power at narrow beam footprint: A laser return must be received by the system above a power threshold to accurately record a measurement. The strength of the laser return (i.e., intensity) is a function of laser emission power, laser footprint, flight altitude and the reflectivity of the target. While surface reflectivity cannot be controlled, laser power can be increased and low flight altitudes can be maintained.

Reduced Scan Angle: Edge-of-scan data can become inaccurate. The scan angle was reduced to a maximum of $\pm 20^\circ$ to $\pm 21^\circ$ from nadir for the green and NIR sensors, respectively. This creates a narrow swath width and greatly reduces laser shadows from trees and buildings.

Quality GPS: Flights took place during optimal GPS conditions (e.g., 6 or more satellites and PDOP [Position Dilution of Precision] less than 3.0). Before each flight, the PDOP was determined for the survey day. During all flight times, a dual frequency DGPS base station recording at 1 second epochs was utilized and a maximum baseline length between the aircraft and the control points was less than 13 nm at all times.

Ground Survey: Ground survey point accuracy (<1.5 cm RMSE) occurs during optimal PDOP ranges and targets a minimal baseline distance of 4 miles between GPS rover and base. Robust statistics are, in part, a function of sample size (n) and distribution. Ground survey points are distributed to the extent possible throughout multiple flight lines and across the survey area.

50% Side-Lap (100% Overlap): Overlapping areas are optimized for relative accuracy testing. Laser shadowing is minimized to help increase target acquisition from multiple scan angles. Ideally, with a 50% side-lap, the nadir portion of one flight line coincides with the swath edge portion of overlapping flight lines. A minimum of 50% side-lap with terrain-followed acquisition prevents data gaps.

Opposing Flight Lines: All overlapping flight lines have opposing directions. Pitch, roll and heading errors are amplified by a factor of two relative to the adjacent flight line(s), making misalignments easier to detect and resolve.







Lower_Platte_Topobathymetric_Lidar_Report_Final_DS

Final Audit Report

2023-03-06

Created:	2023-03-06
By:	Danielle Silver (danielle.silver@nv5.com)
Status:	Signed
Transaction ID:	CBJCHBCAABAAQVr8X0Awn-bTGkGWEmftAXDqF7dKD3Cs

"Lower_Platte_Topobathymetric_Lidar_Report_Final_DS" History

-  Document created by Danielle Silver (danielle.silver@nv5.com)
2023-03-06 - 7:38:15 PM GMT
-  Document emailed to steven.miller@nv5.com for signature
2023-03-06 - 7:40:56 PM GMT
-  Email viewed by steven.miller@nv5.com
2023-03-06 - 7:43:05 PM GMT
-  Signer steven.miller@nv5.com entered name at signing as Steven R. Miller
2023-03-06 - 7:44:06 PM GMT
-  Document e-signed by Steven R. Miller (steven.miller@nv5.com)
Signature Date: 2023-03-06 - 7:44:08 PM GMT - Time Source: server
-  Agreement completed.
2023-03-06 - 7:44:08 PM GMT